



Surface modification of cadmium-based nanoparticles with D-penicillamine—study of pH influence on ligand exchange reaction

A. Lesiak · K. Halicka · M. Chrzanowski · M. Banski · A. Żak · J. Cabaj · A. Podhorodecki

Received: 6 April 2020 / Accepted: 28 July 2020 / Published online: 8 August 2020
© The Author(s) 2020

Abstract Semiconducting nanoparticles (NPs) find applications in many fields, with a recent focus on medicine and biology. Functionalization of the surface of NPs is necessary, and one of the most commonly employed techniques is ligand exchange (LE). In this paper, the study of pH influence on LE reaction for different types of cadmium-based NPs (quantum dots, nanorods, and nanoplates) is presented. Hydrophobic NPs were transferred to the non-organic medium by functionalization with D-penicillamine (DPA). The LE procedure was conducted at four different pH levels (4, 7, 9, and 11), and obtained hydrophilic NPs were dispersed in phosphate buffer. Results show that the most effective procedure resulted from a reaction carried at pH = 4; however, NPs with higher photoluminescence intensity were obtained when pH = 11 was used. Comparable emission was achieved from samples at pH = 4 and pH =

9. The least effective transfer, resulting in unstable NPs, occurred when the procedure was conducted at pH = 7.

Keywords β,β -Dimethylcysteine · Functionalization · Quantum dots · Semiconducting · Thiol-coating

Introduction

Nanoparticles (NPs) are nanoscale semiconducting nanocrystals with specific optical properties, controlled by the size and structure of NPs. This effect is described as the quantum confinement. It can occur in one (nanoplates), two (nanorods), or three dimensions (quantum dots, QDs). Each type of these NPs, due to their unique optical properties, can find application in various fields of science and industry, e.g., for the creation of optoelectronic devices, in bioassays, or in bioimaging (Smith and Nie 2010; Thovhogi et al. 2018; Jamieson et al. 2007; Vasudevan et al. 2015; Klostranec and Chan 2006).

Nowadays, the biomedical field shows a great interest in nanotechnology. Nanoscience can be applied in drug delivery, where NPs serve as nanocarriers or nanodrugs (Zahin et al. 2019); in bioimaging because of the optical properties (e.g., gold NPs can enhance luminescence, QDs can be used for near-infrared imaging, which is desirable for deep-tissue optical imaging); or in biosensors, allowing to achieve a low limit of detection of relevant molecules. However, these applications require adjustment of the properties of NPs, e.g.,

A. Lesiak · K. Halicka · J. Cabaj
Faculty of Chemistry, Wrocław University of Science and Technology, Wybrzeże Wyspińskiego 27, 50-370 Wrocław, Poland

A. Lesiak (✉) · M. Chrzanowski · M. Banski · A. Podhorodecki
Faculty of Fundamental Problems of Technology, Wrocław University of Science and Technology, Wybrzeże Wyspińskiego 27, 50-370 Wrocław, Poland
e-mail: anna.lesiak@pwr.edu.pl

A. Żak
Faculty of Mechanics, Electron Microscopy Laboratory, Wrocław University of Science and Technology, Wybrzeże Wyspińskiego 27, 50-370 Wrocław, Poland

in terms of stability, solubility in aqueous solution, and non-toxicity (Matea et al. 2017). To achieve that, surface modification (functionalization) of NPs is necessary (Blanco-Canosa et al. 2014). This process is based on the binding of (or replacing) chemical or biological molecules to the surface of NPs (Liu and Luo 2014). Functionalization can be performed using several, both chemical and physical, methods, such as ligand exchange (Karakoti et al. 2015; Lim et al. 2016; Wang et al. 2013; Wang et al. 2012; Hu et al. 2016; Smith et al. 2006), silanization (Karakoti et al. 2015; Wang et al. 2012; Zhou et al. 2017), encapsulation in amphiphilic polymer, micellar phospholipid, microsphere, or dendrimeric coatings (Liu and Luo 2014; Wang et al. 2012; Zhou et al. 2017; La Rosa et al. 2017).

The ligand exchange (LE) method is the most common technique used for the stabilization of NPs in aqueous solutions, as it is simple, is fast, and results in non-aggregated particles with preserved size (Smith et al. 2006; La Rosa et al. 2017). This method involves replacing the hydrophobic molecules present on the surface of NPs (e.g., trioctylphosphine (TOP) and its oxide (TOPO), oleic acid (OA)) with molecules (ligands) containing a minimum of two functional groups at opposite ends: first for anchoring to the surface of NPs (usually a thiol group because of its affinity to the surface of NPs (Liu and Luo 2014)) and second for ensuring water solubility (e.g., carboxyl, hydroxyl, amino groups—often occurring in the anionic form) (Karakoti et al. 2015; Lim et al. 2016; Wang et al. 2013; Wang et al. 2012; Hu et al. 2016). The challenge of this method is to obtain a stable shell after the LE. The ligands are in a state of dynamic equilibrium with the solution. Because of that, the existing NP-ligand bond can be broken and replaced with a new one. When a new, different ligand (usually shorter than the initial ligand) is introduced, it competes for the free surface space, affecting the state of equilibrium. To exchange ligands on the surface of NPs, the concentration and surface affinity of the new molecules should be higher than the concentration and affinity of the original ligand (Karakoti et al. 2015). The ligands often used for surface modification to obtain hydrophilic, non-aggregating NPs include polymers (e.g., polyethylene glycol (Liu and Luo 2014; Wenger et al. 2017)), amines, phosphines, or compounds containing thiol groups (Lee et al. 2010) (such as 3-mercaptopropionic acid and its derivatives (Liu and Luo 2014), glutathione (Wang et al. 2012), dihydrolipoic acid (La Rosa et al. 2017)).

Biocompatible molecules are used for functionalization to minimize the toxicity of NPs (Matea et al. 2017).

The presence of ligands on the surface of NPs affects the size, shape, and properties (both optical and physicochemical) of NPs. Surface modification with various ligands allows controlling the colloidal stability of NPs and their dispersion in polar (organic solvents usually used during synthesis) and non-polar environments (e.g., water). The type of attached ligands also determines the possibility of the conjugation of additional biological molecules to the surface of NPs and the reduction of toxicity, making NPs suitable for biomedical applications (Matea et al. 2017; Blanco-Canosa et al. 2014; Zhou et al. 2017). This is why the optimization of the functionalization process is crucial.

This study presents the procedure of preparation of hydrophilic Cd-based NPs (i.e., QDs, nanorods, nanoplates) coated by DPA using a LE method. The experiments were conducted at different pH levels (close to pK_a values of DPA functional groups) to determine optimal conditions for the surface modification process. The results may be potentially applied in further research concerning bioconjugations and biosensors (Lesiak et al. 2019).

Materials and methods

Materials

For NPs' synthesis, the following chemicals were used: cadmium oxide (CdO, 99.5%), selenium (Se, 99.5%), sulfur (S, 99.98%), trioctylphosphine (TOP, 97%), oleic acid (OA, 90%), 1-octadecene (ODE, 90%), trioctylphosphine oxide (TOPO, 90%), octadecylphosphonic acid (ODPA, 99%), hexylphosphonic acid (HPA, 99%), toluene (99.5%), isopropanol (99.5%), methanol (99.9%), cadmium acetate (anhydrous, 99.99%), nonanoic acid ($\geq 96\%$), and 1-octanethiol (99.9%). These chemicals and D-penicillamine (DPA) (99%) used for LE reaction were purchased from Sigma-Aldrich Co. Ethanol (96%), n-hexane (95%), hydrochloric acid (98.5%), sodium hydroxide (98.8%), potassium dihydrogen phosphate, and disodium hydrogen phosphate were purchased from Chempur. All chemicals were used as received without any purification. High-purity water was used throughout all the experiments.

Synthesis of CdS quantum dots

Synthesis of CdS QDs was conducted based on the procedure presented by Čapek et al. (Čapek et al. 2010) with minor changes. For the synthesis of Cd–OA stock solution precursor, 1027 mg of cadmium oxide (8 mmol) and 8 ml of OA (25 mmol) were loaded into a 50-ml three-neck flask, degassed for 10 min at room temperature, and heated to 250 °C. After 30 min, the colorless solution was cooled to 90 °C and 16 ml of ODE was added to prevent solidification. The final solution was degassed under vacuum for 20 min. S–ODE suspension was prepared by mixing 23.7 mg (0.3 mmol) of elemental S powder with 1 ml of ODE. The mixture was sonicated for 10 min and then loaded into the syringe inside the glovebox. To synthesize CdS NPs, a reaction mixture composed of 1.2 ml of Cd–OA stock solution and 18 ml of ODE was degassed for 20 min at room temperature. The temperature of the solution was raised to 240 °C, and then S–ODE suspension was rapidly injected under N₂ atmosphere. The reaction was stopped after 20 min by cooling down the solution. NPs were precipitated with an excess of isopropanol and dispersed in toluene for further analysis.

Synthesis of CdSe/CdS quantum dots

CdSe nanocrystals seeds were synthesized by the heat-up method (Chen et al. 2013). Together with 3.8 ml of ODE and 2 ml of OA, 256.8 mg of cadmium oxide (2 mmol) and 79 mg of selenium (1 mmol) were loaded into a 50-ml three-neck flask and degassed for 30 min at room temperature. After that, the temperature was raised to 240 °C, and nanocrystals' growth proceeded for 10 min. The solution was cooled down, and CdSe seeds were purified three times using isopropanol and then dispersed in cyclohexane at a high concentration of 1.5×10^{-4} mmol/ml, which was determined from the absorbance spectrum.

For the synthesis of CdSe/CdS core-shell NPs, 3×10^{-4} mmol (2 ml) CdSe seeds and 6 ml of ODE were loaded into a 50-ml flask and degassed for 1 h at room temperature to remove the solvent. Then, the temperature was set to 310 °C, and when it raised to 240 °C, 6 ml of Cd–OA solution (1.6 ml of Cd–OA stock solution in ODE) and 6 ml of sulfur precursor (110 µl of 1-octanethiol in ODE) were slowly infused at the rate of 3 ml/h to form CdS shell. After 2 h, shell growth was finished, and the

solution was allowed to slowly cool down to room temperature. CdSe/CdS core-shell nanocrystals were purified using isopropanol and dispersed in toluene.

Synthesis of CdSe/CdS nanorods

Wurtzite CdSe QDs were synthesized following a procedure of Carbone et al. (Carbone et al. 2007). Briefly, TOPO (3 g), CdO (60 mg), and ODPa (280 mg) were loaded into a 50-ml three-neck flask, degassed for 1 h at 150 °C, and then heated to 300 °C under argon atmosphere. After 20 min, the colorless solution was heated to 380 °C and TOP-Se solution (58 mg Se in 360 mg TOP) was injected rapidly. The synthesis was stopped after 30 s and cooled immediately to the temperature of 150 °C, followed by an injection of nonanoic acid (2 ml) and toluene (2 ml) to prevent solidification. CdSe/CdS seeded nanorods were prepared by mixing TOPO (3 g), CdO (60 mg), ODPa (280 mg), and HPA (80 mg) in a flask, followed by degassing at 150 °C for 1 h. The mixture was heated to 300 °C under argon atmosphere and maintained at this temperature for 5 min. Afterward, the temperature was raised to 350 °C and a solution of TOP-S (60 mg S in 1.5 g TOP) and 200 nmol of purified CdSe cores dissolved in TOP (0.5 ml) was rapidly injected. The synthesis proceeded for 8 min, and then the solution was cooled to 150 °C, followed by an injection of toluene (2 ml). Obtained CdSe/CdS nanorods were precipitated with methanol and dispersed in toluene.

Synthesis of CdS nanoplates

CdS nanoplates were prepared based on the procedure described by Ithurria et al. (Ithurria et al. 2011) with minor changes. The following were placed in a flask at room temperature: 424.2 mg cadmium acetate, 26.3 mg sulfur, and 4 ml cadmium oleate (0.4 M) with 20 ml octadecene. The solution was mixed and connected to a vacuum-gas apparatus. The flask was degassed by vacuum-argon exchange for 10 min at room temperature and then set to argon circulation and a thermocouple was connected. Two-stage heating was applied: first, the solution was heated for 20 min at 120 °C, and then, the temperature was increased to 230 °C for 25 min. Obtained CdS nanoplates were dispersed in toluene.

Ligand exchange procedure

Based on the modified literature procedure (Pong et al. 2008; Shen et al. 2013), four reactions of functionalization of NPs using DPA were prepared: CdS QDs, CdSe/CdS QDs, CdSe/CdS nanorods, and CdS nanoplates. Before modification, all NPs had hydrophobic ligands on the surface. As the study aimed to assess the effect of pH on the LE reaction, the pH value of the solution was the only variable in the experiments. First, the aqueous phase was prepared as follows: 10 ml of DPA solution (30.5 mg/ml) in phosphate buffer (pH = 7.4); this solution was then divided into 4 equal parts (2.5 ml each), and each was adjusted to the appropriate pH (pH = 4, pH = 7, pH = 9, and pH = 11, respectively) with 0.1 M HCl or 0.1 M NaOH. Each sample contained 76.25 mg of DPA. To prepare the organic phase, 0.25 ml of the appropriate NPs was added to 3.75 ml of toluene. One milliliter of this mixture was then added to each of the four previously prepared DPA solutions. Samples were shaken for 24 h at room temperature. NPs were purified with ethanol:n-hexane (3:1) mixture using vortex and centrifugation (5 min \times 6000 rpm). These operations were repeated, adding 1 ml of methanol until complete precipitation of NPs from the solution was achieved. The liquid phase from the NP sediment was removed by decantation. The precipitate was dissolved in 1 ml of phosphate buffer (pH = 7.4) and transferred into a vial through a 0.45 μ m PTFE syringe filter.

Quantum dot characterization

Photoluminescence (PL) was induced by 405 nm laser (CNI laser, 1 mW). The emission was collected with an optical fiber, and PL spectra were recorded using CCD spectrometer (AvaSpec-ULS2048XL). Absorbance spectra (ABS) were measured on JASCO V-570 spectrophotometer. Transmission electron microscopy (TEM) was performed on carbon-copper grids on Hitachi H-800 microscope.

Results and discussion

DPA, also called β,β -dimethylcysteine, is a derivative of an amino acid—cysteine (Wilson and Martin 1971). It has three functional groups—carboxyl, amine, and thiol—and corresponding dissociable protonation sites ($pK_{\text{COOH}} = 1.8$, $pK_{\text{NH}_2} = 7.9$, $pK_{\text{SH}} = 10.5$) (Al-Majed et al. 2005). The process of protonation and deprotonation of the amino acids in an aqueous solution depends on the pH level. The ionization process of DPA is presented in Fig. 1 (El Ibrahim et al. 2018). Due to its structure, DPA may participate in such reactions as metal chelation, formation of disulfide bridges, or surface modification of cadmium-based NPs (Al-Majed et al. 2005; Mohammad-Rezaei et al. 2013).

In order to verify the pH-dependent efficiency of the LE process, four experiments were conducted at pH equal to 4, 7, 9, and 11. Due to the protonation of functional groups, which depends on the pK_a value, and thus on the pH of the solution, examples of values corresponding to individual forms of the DPA molecule were selected. The experiment was not carried out at pH lower than the pK_a of the carboxyl group because a strongly acidic environment could break down the structure of investigated materials (Aldana et al. 2005).

Experimental pH of DPA solution was measured and amounted to 6.6. The pH level of the aqueous phase was adjusted to 4 by adding 0.1 M HCl and to 7, 9, or 11 by adding 0.1 M NaOH. On top of the non-organic phase, an organic phase was formed by placing OA-capped NPs dispersed in toluene and the LE procedure was conducted.

Figure 2a–d shows collected ABS and PL spectra of Cd-based NPs before surface modification. As can be seen, CdS QDs, CdSe/CdS QDs, and CdSe/CdS nanorods were characterized by the presence of PL emission that was not significantly affected by defects states. However, in the case of CdS nanoplates, there was no emission detected, due to typical for this geometry high surface area and a number of defects present at the surface (Tessier et al. 2013).

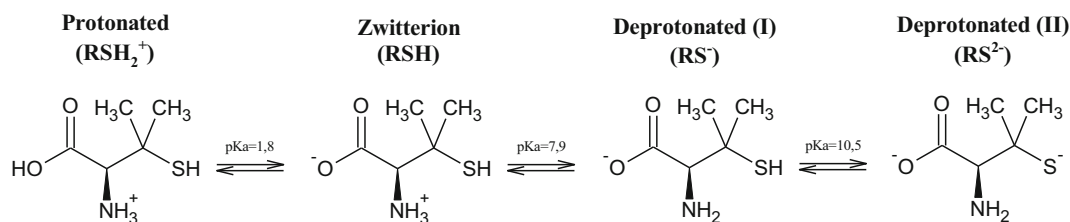
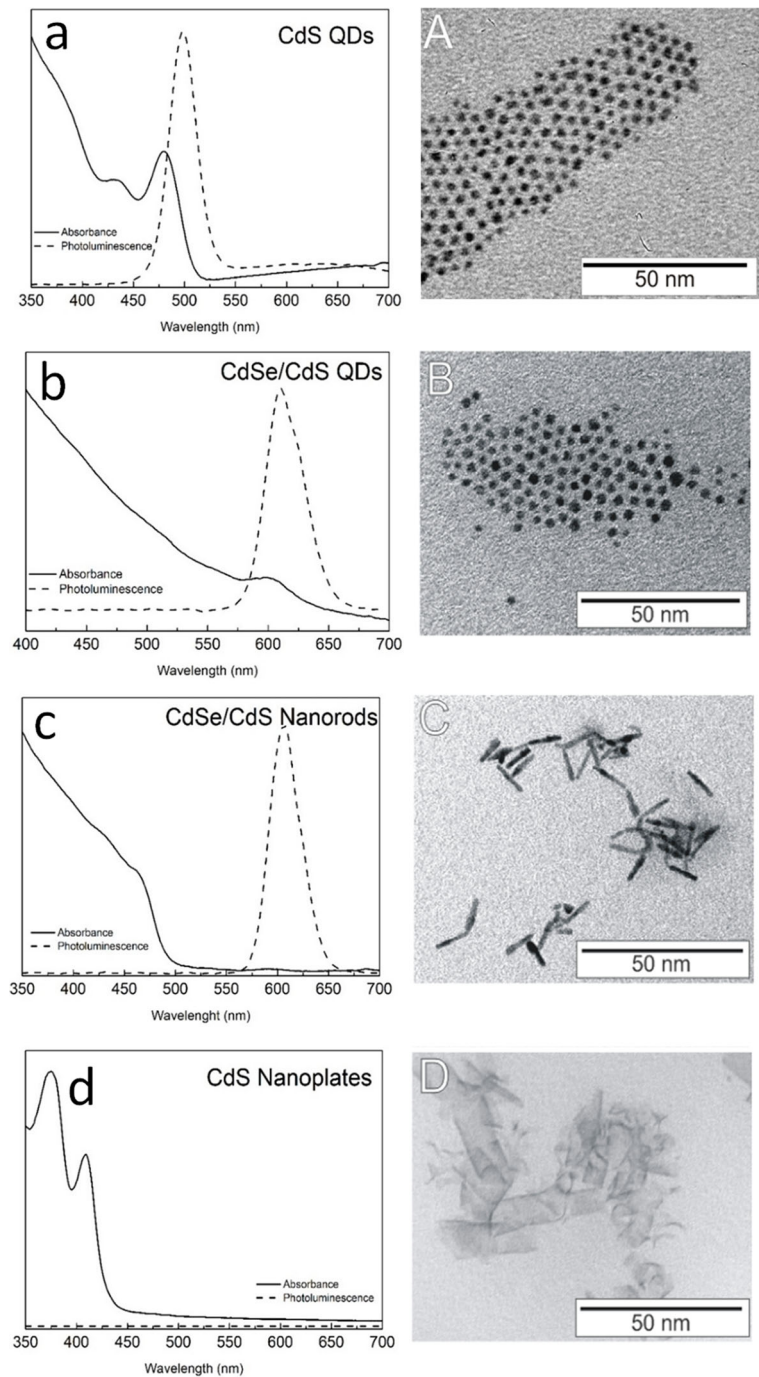


Fig. 1 DPA ionization at different pH levels of the aqueous medium

Fig. 2 (a–d) ABS and PL spectra and (A–D) TEM pictures of NPs before surface modification: (a, A) CdS QDs. (b, B) CdSe/CdS QDs. (c, C) CdSe/CdS nanorods. (d, D) CdS nanoplates



The variety of NPs used was confirmed (El-Bially et al. 2012; Adel et al. 2017; Kormilina et al. 2017) by TEM measurements (Fig. 2 A–D). The morphological display of NPs showed that they were nearly homogeneous and monodisperse. Spherical in shape CdS QDs and CdSe/CdS QDs had sizes approximately 2.5 nm and

4.5 nm, respectively. The average length of CdS nanorods was 10 nm. CdS nanoplates had a size of approximately 10×18 nm and the thickness of a single monolayer. This could cause interactions, resulting in the NPs “rolling-up,” which was observed especially along the shorter axis of NPs.

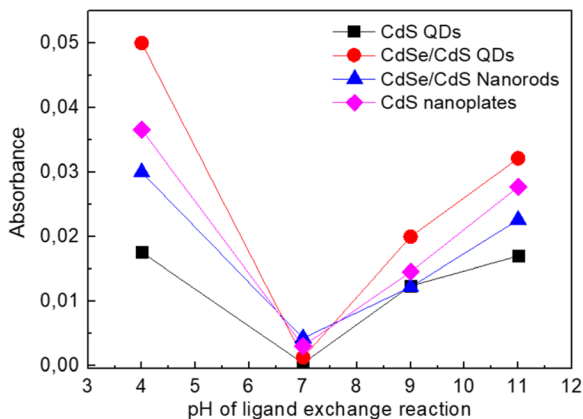


Fig. 3 Absorbance of DPA-coated NPs after LE reaction conducted under various pH conditions

The measurements were performed for DPA-coated NPs, after the LE reaction as well (Fig. 3). It was observed that the most efficient transfer of ligands during the LE process occurred at pH = 4. When the LE procedure was performed under alkaline conditions, it was noticed that a more recommended solution for phase transfer was containing a higher concentration of OH⁻ ion (pH = 11). pH = 7 was the least preferred environment during LE. It may be explained by the fact that during the LE performed at pH = 7, DPA occurs in a relatively high concentration (compared to the reaction at pH = 4) in the form of a zwitterion, and in this form amino acids have the lowest solubility (Howard-Lock et al. 1991). Additionally, NPs functionalized at pH = 7 were not stable in time. The aggregates of NPs appeared 1 day after the LE process and were visible without specific apparatus (an example of CdSe/CdS nanorods is shown in Fig. 4). After mixing, they underwent a total dispersion in an aqueous medium. All samples after LE were transferred to the phosphate buffer (pH = 7.4), which—in case of the samples

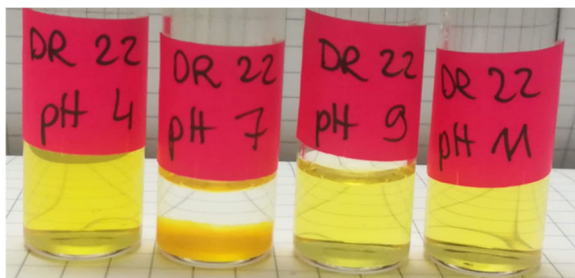


Fig. 4 CdSe/CdS nanorods in phosphate buffer (pH = 7.4) after the LE reaction. Labels on the vials describe pH value during modification process

prepared in similar conditions—could promote enhancement of the zwitterionic form of the ligand. Breus et al. discovered that longer exposure to mixing conditions during the LE reaction (under conditions in which ligand molecule takes the form of a zwitterion) may lead to additional reaction between ionic forms of carboxylic and amino groups of different DPA molecules, resulting in dissociation of the ligand from the surface of NPs. The LE reaction in the conducted experiment was carried out for 24 h, which might have influenced the precipitation of NPs during storage (Breus et al. 2009).

The presence of DPA on the surface of NPs influenced their PL properties. Based on the results presented in Fig. 5, it can be concluded that despite the more effective LE conducted at pH = 4 (proving that more NPs passed into the aqueous medium), higher PL intensity was observed for CdSe/CdS QDs and CdSe/CdS nanorods if the transfer reactions were carried at pH = 11. Moreover, the samples of NPs obtained at pH = 4 and pH = 9 showed comparable emission. For CdS QDs samples, regardless of the LE conditions, no PL emission after the process was noticed. In the case of CdS QDs, the phase transfer promotes new defect formation on the surface of QDs. This enhances nonradiative recombination processes and reflects in quenching of the emission intensity (Spanhel et al. 1987). Based on obtained results, it can be concluded that during the LE process for core-shell structures (CdSe/CdS QDs, CdSe/CdS nanorods) run under extremely alkaline conditions (pH = 11), lower chemical interference in the structure occurs, which causes fewer defects (than under acidic conditions), i.e., higher PL emission values.

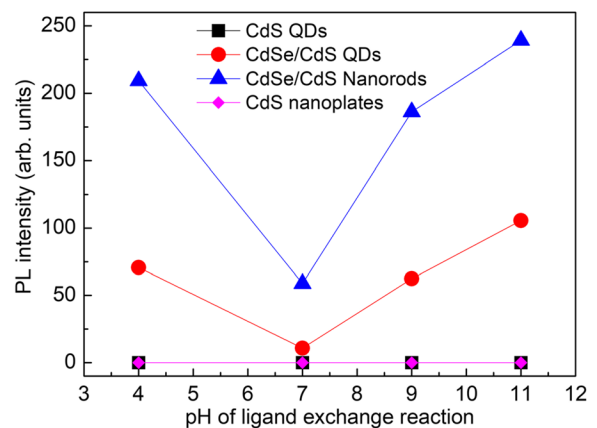


Fig. 5 PL intensity of DPA-coated NPs after LE reaction conducted under various pH conditions.

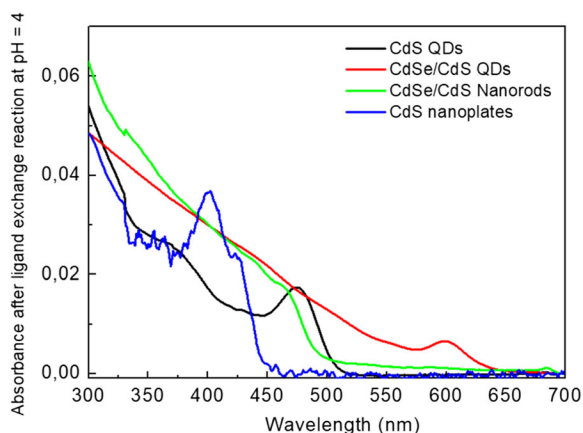


Fig. 6 Absorbance spectra after the LE reaction conducted at pH = 4

Since the most effective LE reaction was observed at pH = 4, representative absorbance spectra for NPs modified under these conditions are presented in Fig. 6. Comparing the absorbance results obtained for CdS QDs, CdSe/CdS QDs, and CdSe/CdS nanorods before and after DPA-coating, no significant influence on the shape of the spectra by the process can be observed. However, for CdS nanoplates, the LE induced evident changes in the absorption spectrum: before LE reaction, two absorption peaks were observed (375 nm and 410 nm); after DPA coating, only one absorption peak, with maximum absorbance at 402 nm, was observed. It suggests that during the surface modification with DPA, the distribution of nanoplate thickness was improved and the bi-modal distribution (5 and 6 monolayers) was converted to a single-mode distribution (6 monolayers) (Ithurria et al. 2011). However, due to the complexity of this scientific problem, deeper discussion on these results is out of the scope of this paper and will be reported elsewhere.

Conclusions

The influence of pH conditions on the LE process for different types of semiconducting Cd-based NPs was investigated. LE procedure was performed at various pH levels (4, 7, 9, 11), and in result, hydrophilic NPs coated by DPA were obtained. The results show that regardless of the structure of NPs, the surface modification occurs to a small extent or does not occur at all, if neutral conditions (pH = 7) are applied, giving the least stable NPs. Additionally, it can be concluded that although the

most NPs was successfully transferred under acidic conditions, an increase in PL intensity was observed at the highest concentrations of OH⁻ ions (pH 11).

NPs obtained in the experiment can later be bioconjugated to various biomolecules in a reaction influenced by the pH level. NPs-biomolecule complexes can find biomedical and sensory applications.

Acknowledgements The authors acknowledge the National Science Centre for their financial support within the Sonata 8 project no. UMO-2014/15/ D/ST5/02744.

Compliance with ethical standards

Conflict of interest The authors declare that they have no conflict of interest.

Open Access This article is licensed under a Creative Commons Attribution 4.0 International License, which permits use, sharing, adaptation, distribution and reproduction in any medium or format, as long as you give appropriate credit to the original author(s) and the source, provide a link to the Creative Commons licence, and indicate if changes were made. The images or other third party material in this article are included in the article's Creative Commons licence, unless indicated otherwise in a credit line to the material. If material is not included in the article's Creative Commons licence and your intended use is not permitted by statutory regulation or exceeds the permitted use, you will need to obtain permission directly from the copyright holder. To view a copy of this licence, visit <http://creativecommons.org/licenses/by/4.0/>.

References

- Adel P, Bloh J, Hinrichs D, Kodanek T, Dorfs D (2017) Determination of all dimensions of CdSe seeded CdS nanorods solely via their UV/Vis spectra. *Z Phys Chem* 231(1): 93–106. <https://doi.org/10.1515/zpch-2016-0887>
- Aldana J, Lavelle N, Wang Y, Peng X (2005) Size-dependent dissociation pH of thiolate ligands from cadmium chalcogenide nanocrystals. *J Am Chem Soc* 127:2496–2504. <https://doi.org/10.1021/ja047000+>
- Al-Majed A, Belal F, Julkhuf S, El-Subbagh H (2005) Penicillamine: physical profile. In: Brittain HG (ed) Profiles of drug substances, excipients and related methodology, Vol 32. Elsevier, San Diego, pp 119–130
- Blanco-Canosa JB, Wu M, Susumu K, Petryayeva E, Jennings TL, Dawson PE, Algar WR, Medintz IL (2014) Recent progress in the bioconjugation of quantum dots. *Coord Chem Rev* 263–264:101–137. <https://doi.org/10.1016/j.ccr.2013.08.030>
- Breus VV, Heyes CD, Tron K, Nienhaus GU (2009) Zwitterionic biocompatible quantum dots for wide pH stability and weak nonspecific binding to cells. *ACS Nano* 3(9):2573–2580. <https://doi.org/10.1021/nn900600w>

- Čapek RK, Moreels I, Lambert K, De Muynck D, Zhao Q, Van Tomme A, Vanhaecke F, Hens Z (2010) Optical properties of zincblende cadmium selenide quantum dots. *J Phys Chem C* 114:6371–6376. <https://doi.org/10.1021/jp1001989>
- Carbone L, Nobile C, De Giorgi M, Sala FD, Morello G, Pompa P, Hytch M, Snoeck E, Fiore A, Franchini IR, Nadasan M, Silvestre AF, Chiodo L, Kudera S, Cingolani R, Krahne R, Manna L (2007) Synthesis and micrometer-scale assembly of colloidal CdSe/CdS nanorods prepared by a seeded growth approach. *Nano Lett* 7(10):2942–2950. <https://doi.org/10.1021/nl0717661>
- Chen O, Zhao J, Chauhan VP, Cui J, Wong C, Harris DK, Wie H, Han H-S, Fukumura D, Jain RK, Bawendi MG (2013) Compact high-quality CdSe–CdS core–shell nanocrystals with narrow emission linewidths and suppressed blinking. *Nat Mater* 12:445–451. <https://doi.org/10.1038/nmat3539>
- El Ibrahimy B, Jmiai A, Somoue A, Oukhrif R, Chadili M, El Issami S, Bazzi L (2018) Cysteine duality effect on the corrosion inhibition and acceleration of 3003 aluminium alloy in a 2% NaCl solution. *Port Electrochim Acta* 36(6): 403–422. <https://doi.org/10.4152/pea.201806403>
- El-Bially AB, Seoudi R, Eisa W, Shabaka AA, Soliman SI, Abd El-Hamid RK, Ramadan RA (2012) Preparation, characterization and physical properties of CdS nanoparticles with different sizes. *J Appl Sci Res* 8(2):676–685
- Howard-Lock HE, Lock CJL, Martins ML (1991) Amino acid/zwitterion equilibria 11: vibrational and NMR studies of substituted thiazolidine-4-carboxylic acids. *Can J Chem* 69: 1721–1727. <https://doi.org/10.1139/v91-252>
- Hu L, Zhang C, Zeng G, Chen G, Wan J, Guo Z, Wu H, Yu Z, Zhou Y, Liu J (2016) Metal-based quantum dots: synthesis, surface modification, transport and fate in aquatic environments and toxicity to microorganisms. *RSC Adv* 6:78595–78610. <https://doi.org/10.1039/C6RA13016J>
- Ithurria S, Tessier MD, Mahler B, Lobo RPSM, Dubertret B, Efros AL (2011) Colloidal nanoplatelets with two-dimensional electronic structure. *Nat Mater* 10(12):936–941. <https://doi.org/10.1038/nmat3145>
- Jamieson T, Bakhshi R, Petrova D, Pocock R, Imani M, Seifalian AM (2007) Biological applications of quantum dots. *Biomaterials* 28:4717–4732. <https://doi.org/10.1016/j.biomaterials.2007.07.014>
- Karakoti AS, Shukla R, Shanker R, Singh S (2015) Surface functionalization of quantum dots for biological applications. *Adv Colloid Interfac* 215:28–45. <https://doi.org/10.1016/j.cis.2014.11.004>
- Klostranec JM, Chan WCW (2006) Quantum dots in biological and biomedical research: recent progress and present challenges. *Adv Mater* 18:1953–1964. <https://doi.org/10.1002/adma.200500786>
- Kormilina TK, Cherevkov SA, Fedorov AV, Baranov AV (2017) Cadmium chalcogenide nano-heteroplatelets: creating advanced nanostructured materials by shell growth, substitution, and attachment. *Small* 13(41):1702300. <https://doi.org/10.1002/sml.201702300>
- La Rosa M, Avellini T, Lincheneau C, Silvi S, Wright IA, Constable EC, Credi A (2017) An efficient method for the surface functionalization of luminescent quantum dots with lipoic acid based ligands. *Eur J Inorg Chem* 2017(44):5143–5151. <https://doi.org/10.1002/ejic.201700781>
- Lee CM, Jang DR, Cheong SJ, Kim EM, Jeong MH, Kim SH, Kim DW, Lim ST, Sohn MH, Jeong HJ (2010) Surface engineering of quantum dots for in vivo imaging. *Nanotechnology* 21(28):285102. <https://doi.org/10.1088/0957-4484/21/28/285102>
- Lesiak A, Drzozga K, Cabaj J, Bański M, Malecha K, Podhorodecki A (2019) Optical sensors based on II–VI quantum dots. *Nanomaterials* 9(2):192. <https://doi.org/10.3390/nano9020192>
- Lim SJ, Ma L, Schleife A, Smith AM (2016) Quantum dot surface engineering: toward inert fluorophores with compact size and bright, stable emission. *Coord Chem Rev* 320–321:216–237. <https://doi.org/10.1016/j.ccr.2016.03.012>
- Liu X, Luo Y (2014) Surface modifications technology of quantum dots based biosensors and their medical applications. *Chin J Anal Chem* 42(7):1061–1069. [https://doi.org/10.1016/S1872-2040\(14\)60753-2](https://doi.org/10.1016/S1872-2040(14)60753-2)
- Matea CT, Mocan T, Tabaran F, Pop T, Mosteanu O, Puia C, Iancu C, Mocan L (2017) Quantum dots in imaging, drug delivery and sensor applications. *Int J Nanomedicine* 12: 5421–5431. <https://doi.org/10.2147/IJN.S138624>
- Mohammad-Rezaei R, Razmi H, Abdolmohammad-Zadeh H (2013) D-penicillamine capped cadmium telluride quantum dots as a novel fluorometric sensor of copper(II). *Luminescence* 28(4):503–509. <https://doi.org/10.1002/bio.2484>
- Pong B-K, Trout BL, Lee J-Y (2008) Modified ligand-exchange for efficient solubilization of CdSe/ZnS quantum dots in water: a procedure guided by computational studies. *Langmuir* 24:5270–5276. <https://doi.org/10.1021/la703431j>
- Shen Y, Gee MY, Tan R, Pellechia PJ, Greytak AB (2013) Purification of quantum dots by gel permeation chromatography and the effect of excess ligands on shell growth and ligand exchange. *Chem Mater* 25(14):2838–2848. <https://doi.org/10.1021/cm4012734>
- Smith AM, Nie S (2010) Semiconductor nanocrystals: structure, properties, and band gap engineering. *Acc Chem Res* 43(2): 190–200. <https://doi.org/10.1021/ar9001069>
- Smith AM, Duan H, Rhyner MN, Ruan G, Nie S (2006) A systematic examination of surface coatings on the optical and chemical properties of semiconductor quantum dots. *Phys Chem Chem Phys* 8:3895–3903. <https://doi.org/10.1039/B606572B>
- Spanhel L, Haase M, Weller H, Henglein A (1987) Photochemistry of colloidal semiconductors. 20. Surface modification and stability of strong luminescing CdS particles. *J Am Chem Soc* 109(19):5649–5655. <https://doi.org/10.1021/ja00253a015>
- Tessier MD, Spinicelli P, Dupont D, Patriarche G, Ithurria S, Dubertret B (2013) Efficient exciton concentrators built from colloidal Core/crown CdSe/CdS semiconductor nanoplatelets. *Nano Lett* 14(1):207–213. <https://doi.org/10.1021/nl403746p>
- Thovhogi N, Sibuyi NRS, Onani MO, Meyer M, Madiehe AM (2018) Peptide-functionalized quantum dots for potential applications in the imaging and treatment of obesity. *Int J Nanomedicine* 13:2551–2559. <https://doi.org/10.2147/IJN.S158687>
- Vasudevan D, Gaddam RR, Trinchi A, Cole I (2015) Core–shell quantum dots: properties and applications. *J Alloy Compd* 636:395–404. <https://doi.org/10.1016/j.jallcom.2015.02.102>

- Wang J, Han S, Ke D, Wang R (2012) Semiconductor quantum dots surface modification for potential cancer diagnostic and therapeutic applications. *J Nanomater* 2012:129041–129048. <https://doi.org/10.1155/2012/129041>
- Wang S, Zhou C, Yuan H, Shen H, Zhao W, Ma L, Li LS (2013) A robust ligand exchange approach for preparing hydrophilic, biocompatible photoluminescent quantum dots. *Mater Res Bull* 48:2836–2842. <https://doi.org/10.1016/j.materresbull.2013.04.015>
- Wenger WN, Bates FS, Aydil ES (2017) Functionalization of cadmium selenide quantum dots with poly(ethylene glycol): ligand exchange, surface coverage, and dispersion stability. *Langmuir* 33:8239–8245. <https://doi.org/10.1021/acs.langmuir.7b01924>
- Wilson EW, Martin RB (1971) Penicillamine deprotonations and interactions with copper ions. *Arch Biochem Biophys* 142(2):445–454. [https://doi.org/10.1016/0003-9861\(71\)90508-x](https://doi.org/10.1016/0003-9861(71)90508-x)
- Zahin N, Anwar R, Tewari D, Kabir T, Sajid A, Mathew B, Uddin S, Aleya L, Abdel-Daim M (2019) Nanoparticles and its biomedical applications in health and diseases: special focus on drug delivery. *Environ Sci Pollut Res* 27:19151–19168. <https://doi.org/10.1007/s11356-019-05211-0>
- Zhou J, Liu Y, Tang J, Tang W (2017) Surface ligands engineering of semiconductor quantum dots for chemosensory and biological application. *Mater Today* 20(7):360–376. <https://doi.org/10.1016/j.mattod.2017.02.006>

Publisher's note Springer Nature remains neutral with regard to jurisdictional claims in published maps and institutional affiliations.